CHEMISTRY
A EUROPEAN JOURNAL

FULL PAPER

DOI: 10.1002/chem.201103932

Structure–Activity Studies on the Fluorescent Indicator in a Displacement Assay for the Screening of Small Molecules Binding to RNA

Shiori Umemoto,[a] Seongwang Im,[a] Jinhua Zhang,[a] Masaki Hagihara,[a] Asako Murata,[a] Yasue Harada,[a] Takeo Fukuzumi,[a] Takahiro Wazaki,[b] Shin-ichi Sasaoka,[b] and Kazuhiko Nakatani*[a]

Abstract: A series of xanthone and thioxanthone derivatives with aminoalkoxy substituents were synthesized as fluorescent indicators for a displacement assay in the study of small-molecule–RNA interactions. The RNA-binding properties of these molecules were investigated in terms of the improved binding selectivity to the loop region in the RNA secondary structure relative to 2,7-bis(2-aminoethoxy)xanthone (X2S) by fluorimetric titration and displacement assay. An 11-mer double-stranded RNA and a hairpin RNA mimicking the stem loop IIB of Rev response element (RRE) RNA of HIV-1 mRNA were used. The X2S derivatives with longer aminoalkyl substituents showed a higher affinity to the double-stranded RNA than the parent molecule. Introduction of a methyl group on the aminoethoxy moiety of X2S effectively modulated the selectivity to the RNA secondary structure. Methyl group substitution at the C1′ position suppressed the binding to the loop regions. Substitution with two methyl groups on the amino nitrogen atom resulted in reducing the affinity to the double-stranded region by a factor of 40%. The effect of methyl substitution on the amino nitrogen atom was also observed for a thioxanthone derivative. Titration experiments, however, suggested that thioxanthone derivatives showed a more prominent tendency of multiple binding to RNA than xanthone derivatives. The selectivity index calculated from the affinity to the double-stranded and loop regions suggested that the *N*,*N*-dimethyl derivative of X2S would be suitable for the screening of small molecules binding to RRE.

Keywords: displacement assay · fluorescent probes · RNA · small molecules · xanthones

Introduction

A displacement assay is a method to investigate the interactions between two molecules, for example, ligand and receptor, by monitoring a signal produced from the indicator, an auxiliary molecule added as a reporter.[1–5] When the indicator and test molecules compete for the same binding site on the receptor, the test molecule can replace the indicator bound to the receptor. The necessary character of the indicator in a displacement assay is to change signals unique to the indicator, such as absorption and fluorescence, depending on its bound and free states. In particular, an assay using a change of indicator fluorescence is called a fluorescent indicator displacement (FID) assay (Figure 1). In the depicted FID assay, the fluorescence of the indicator is quenched upon binding to the receptor. Displacement of the bound indicator with test molecules results in the increase of the fluorescence intensity emitted from the free unbound indicator.

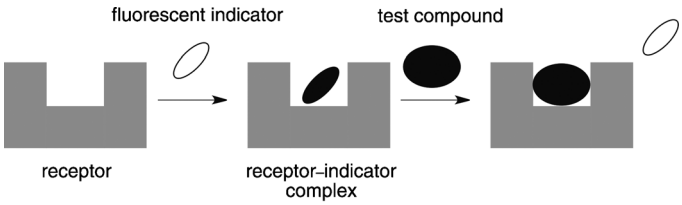

Figure 1. Illustration of the FID assay.

Among methods to investigate molecular interactions, the displacement assay is characterized by a simple procedure. Neither labeling nor immobilization of receptor on the solid support is necessary for the assay. Covalent modification with fluorescent labels and surface immobilization intrinsically hold possibilities leading to an unnatural folding and structure of receptors. The subsequent assay may investigate the binding of molecules to the unnatural structures. In con-

[a] Dr. S. Umemoto, S. Im, Dr. J. Zhang, Dr. M. Hagihara, Dr. A. Murata, Y. Harada, Dr. T. Fukuzumi, Prof. Dr. K. Nakatani
Department of Regulatory Bioorganic Chemistry
The Institute of Scientific and Industrial Research, Osaka University
8-1 Mihogaoka, Ibaraki 567-0047 (Japan)
Fax: (+81) 6-6879-8459
E-mail: nakatani@sanken.osaka-u.ac.jp

[b] T. Wazaki, S. Sasaoka
Research & Development Division
Nitto Kasei Co., Ltd.
17-14 Nishiawaji 3-Chome, Higashiyodogawa-Ku, Osaka 533-0031 (Japan)

Supporting information for this article is available on the WWW under http://dx.doi.org/10.1002/chem.201103932.

trast, the displacement assay can be performed in a homogeneous solution in the presence of the indicator without any covalent modification of the target. Another important characteristic of the displacement assay is scalability of the assay format from small to large compound libraries without much difficulty. The preparation of a large quantity of fluorescently labeled proteins and nucleic acids is still problematic and high in cost, but a displacement assay uses the natural unlabeled proteins and nucleic acids, which could be supplied by cell-free translation and chemical synthesis or transcription.

The drawback to the displacement assay is that the observed signal is not directly produced from the binding of the test molecule to the receptor, but indirectly produced from the dissociation of the indicator bound to the receptor. The quality of the displacement assay regarding the accuracy in the molecular interaction, therefore, would be high when the indicator and the test ligand competitively bind to the receptor. In a real situation, however, the binding among three molecules (e.g., indicator, receptor, and test molecule) might involve unnecessary binary (e.g., indicator–ligand) and ternary (receptor–indicator–ligand) molecular interactions besides the expected ligand–receptor interaction. Nonspecific binding of the indicator to the receptor leading to multiple binding of the indicator also decreases the quality of the assay data. In other words, the quality of the displacement assay depends on the binding properties of the indicator to the receptor.

We have recently reported an FID assay using 2,7-bis(2-aminoethoxy)xanthone (X2S, **3a**) as a fluorescent indicator for the study of the ligand–RNA interaction,[5] because small molecules interacting with biologically important RNA structures have been envisioned as potential drug candidates.[6] We found that the fluorescence of X2S is intense when the X2S is free in solution but is quenched when it is bound to RNA. Fluorimetric titration of X2S with double-stranded RNA (dsRNA), RNA with a single nucleotide bulge, and a model RNA of stem loop IIb in Rev response element (RRE) of HIV-1 mRNA[7] showed that X2S favorably bound to stem loops with some selectivity. Displacement experiments with a model peptide of Rev protein showed that X2S competitively bound to RRE with Rev peptide. RRE is an important secondary structure of HIV-1 mRNA, and is the site for the binding to Rev protein. Rev binding to RRE is essential for the nuclear export of the full-length HIV-1 mRNA to cytoplasm without splicing.[7,8] Small molecules binding to RRE and suppressing the Rev binding were anticipated as potential therapeutics for HIV-1 proliferation.[9] X2S was applied to the screening of small molecular ligands binding to RRE from the LOPAC1280 chemical library. The displacement assay against RRE with X2S as a fluorescent indicator showed that mitoxantrones[10] and sanguinarine[11] were suggested to bind to RRE, and the binding was confirmed separately by isothermal titration calorimetry analysis.

We learned from the screening studies with X2S that fluorescent indicators with higher structural selectivity to the stem loop region than X2S would improve the assay quality by eliminating the nonspecific binders, for example, molecules binding to dsRNA. Because the loop structures are more prominent sites of protein binding than the double-stranded region,[12] fluorescent indicators having weak affinity to the double-stranded region and a binding preference to the stem loop structures would be suitable for the screening of small molecules that potentially modulate the RNA–protein interaction. We realized that another issue in FID is the overlap of the fluorescence spectra of X2S with those of library compounds. A library compound with emitting fluorescence that is overlapped with the fluorescence of the indicator could not be correctly assessed by the FID assay. Under normal screening conditions, the concentration of the library compounds is usually much higher than that of the indicator. In our screening of the LOPAC1280 chemical library with X2S, we first eliminated 59 compounds that emit fluorescence about three times stronger than X2S. On the basis of these discussions on our previous screening studies by FID assay, herein we report studies on a series of xanthone derivatives to look for improved binding selectivity to the stem loop region relative to X2S and thioxanthone derivatives emitting fluorescence at a longer wavelength.[13] We found that introduction of two methyl groups on a primary amino group in X2S to give a dimethylamino group significantly improved the selective binding to the loop region over the binding to the double-stranded region, and that the thioxanthone derivative showing fluorescence with an approximately 45 nm shift to a longer wavelength was also useful for the FID assay.

Results and Discussion

Synthesis of X2S derivatives: We synthesized a series of X2S derivatives with respect to the length of the linker, from three methylene groups **3b** ($n=3$) to six methylene groups **3e** ($n=6$; Figure 2). Syntheses of these compounds were carried out by Mitsunobu reaction of 2,7-dihydroxyxanthone (**1**)[14] with the appropriate *tert*-butoxycarbonyl (Boc)-protected amino alcohols followed by deprotection with an acidic treatment (Scheme 1). By using the same procedure, we also synthesized X2S derivatives **3g** and **3f**, containing a methyl substituent at the aminoethoxy moiety as a mixture of diastereoisomers, and *N,N*-disubstituted **4**, containing two methyl groups at the amino nitrogen atom. Thioxanthone is known to emit fluorescence at a longer wavelength than xanthone. Therefore, 2,7-Bis(2-aminoethoxy)thioxanthone (**5**) and its *N,N*-dimethyl derivative **6** were synthesized from 2,7-dihydroxythioxanthone[15] by Mitsunobu reaction. NMR spectra of the synthesized compounds are shown in the Supporting Information.

Photochemical properties of X2S derivatives: The absorption and emission spectra of X2S derivatives were measured in a buffered solution at pH 7. The X2S derivatives having different linker lengths (**3a–e**) showed a slight deviation in

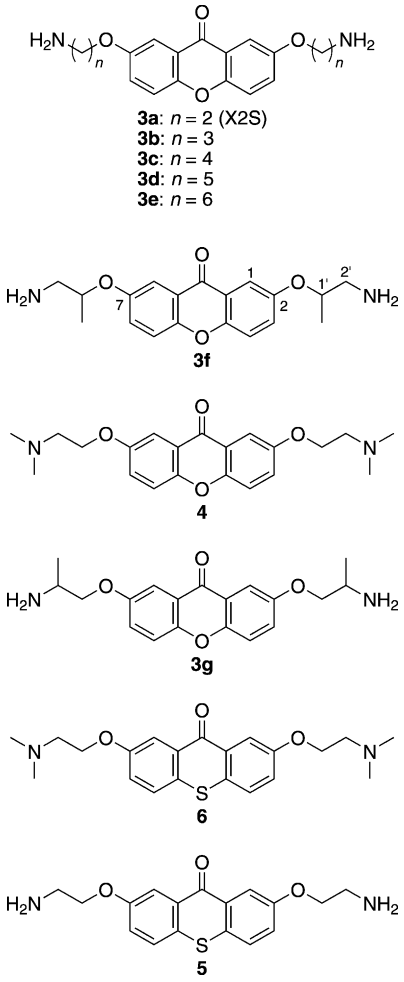

Figure 2. The xanthone and thioxanthone derivatives studied as indicators for the FID assay.

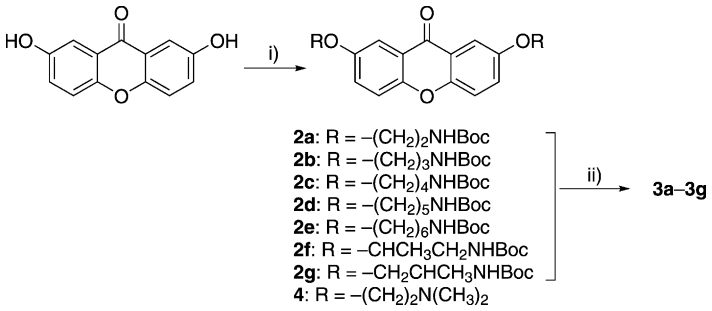

Scheme 1. Synthesis of xanthones **3a**–**g** and **4**. i) Ph_3P, diethyl azodicarboxylate (DEAD), Boc-protected amino alcohol, THF; ii) 4 N HCl/EtOAc.

the absorption maximum (Table 1). The absorption maximum of **3a** was 370 nm, whereas that of **3e** was 377 nm. The emission maximum of X2S derivatives also showed a shift depending on the linker length (Figure 3). The fluorescence spectra of **3a** showed an emission peak at 450 nm, whereas **3d** and **e** showed the peak at the longest wavelength of 464 nm. The fluorescence quantum yield of **3a** was 0.73, the highest among these five compounds. Introduction of the methyl group into the linker did not result in a significant shift of the absorption and emission wavelengths. Compounds **3f** and **3g** with methyl substitution at the C1′ and C2′ position in the linker, respectively, showed absorption and emission maxima at 370 and 455 nm for **3f** and 370 and 452 nm for **3g**. *N*,*N*-Dimethyl derivative **4** also showed similar spectral properties. The fluorescence quantum yield of **3f** and **3g** was 0.75 and 0.76, respectively, showing a slightly higher value than **3a**, although substitution with two methyl groups at nitrogen in compound **4** led to a decrease in the fluorescence quantum yield to 0.66. Thioxanthone derivative **5** and its *N*,*N*-dimethyl derivative **6** showed almost identical spectra with the absorption maximum at 424 nm and emis-

Table 1. Absorption and fluorescence properties of xanthone and thioxanthone derivatives.

	3a	3b	3c	3d	3e	3f	3g	4	5	6
λ_{ex}	370	372	372	376	377	370	370	370	424	424
λ_{em}	450	457	463	464	464	455	452	451	496	493
φ_f	0.73	0.70	0.68	0.67	0.65	0.75	0.76	0.66	0.55	0.49

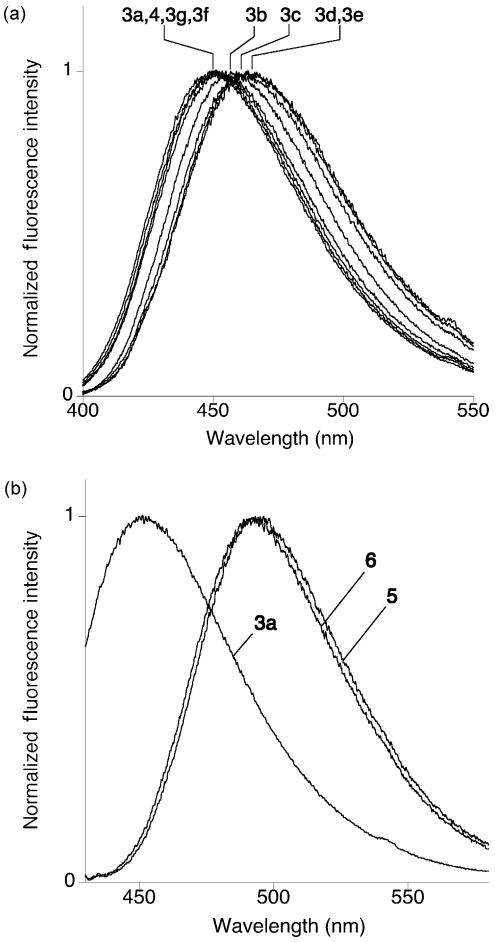

Figure 3. Normalized fluorescence spectra of a) xanthones **3a**–**4** and b) thioxanthones **5** and **6** in sodium cacodylate buffer (pH 7, 10 mM) and NaCl (100 mM). Data for **3a** are shown in b) for comparison.

sion maximum at around 495 nm. The fluorescence quantum yields of **5** and **6** were 0.55 and 0.49, respectively.

Fluorescence quenching by RNA: Fluorimetric titration of X2S derivatives was investigated with an 11-mer fully complementary dsRNA and a hairpin RNA mimicking RRE stem loop IIb (hpRNA; Figure 4).[4a] The relative fluorescence intensities of X2S derivatives of different linker length (**3a–e**) titrated with dsRNA and hpRNA are shown in Figure 5. The efficiency of fluorescence quenching of X2S

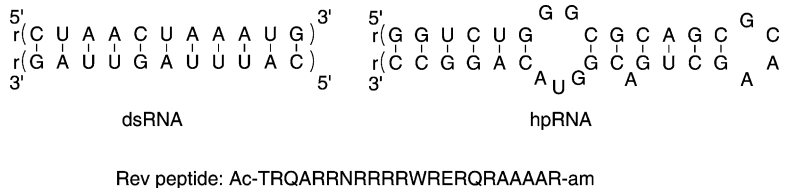

Figure 4. The sequence and secondary structure of dsRNA, hpRNA, and Rev peptide used in these studies.

derivatives by dsRNA was highly dependent on the linker length (Figure 5a). In the presence of an equimolar amount of dsRNA, the fluorescence intensity of **3a** was still 73% that of intact **3a**, whereas that of **3e** in the presence of dsRNA was reduced to 21%. The fluorescence quenching by dsRNA became more efficient as the linker length increased. In contrast, the fluorescence intensities of these compounds titrated with hpRNA were not markedly different from each other.

The titration plots obtained with dsRNA were analyzed by assuming static quenching with a 1:1 binding stoichiometry, represented by Equation (1), in which the relative fluorescence intensity F/F_0 is described by the free dsRNA concentration [RNA] and the apparent dissociation constant K_d(ds) of the dsRNA–indicator complex. The titration data with dsRNA were fitted to Equation (1) by the least-squares curve-fitting method with the coefficient of determination (R^2) being higher than 0.96 (Figure 5). K_d(ds) values for the complexes of dsRNA with **3a–e** obtained by least-squares curve fitting were 1.7×10^{-6}, 5.7×10^{-7}, 4.0×10^{-7}, 1.8×10^{-7}, and 3.7×10^{-8} M, respectively (Table 2). The titration data obtained with hpRNA, however, could not be fitted by Equation (1) with a good coefficient of determination, most likely due to the binding of X2S derivatives simultaneously to both the double-stranded and loop regions.

$$\frac{F}{F_0}=\frac{K_d(\mathrm{ds})}{K_d(\mathrm{ds})+[\mathrm{RNA}]} \quad (1)$$

Alternatively, we used the binding model for the evaluation of the binding to hpRNA,[16] in which the indicator binds independently to the double-stranded and loop regions with a 1:1 binding stoichiometry to each region. The relative fluorescence intensity obtained by titrating with hpRNA is described by Equation (2), in which K_d(ds) and K_d(loop) represent the apparent dissociation constant of

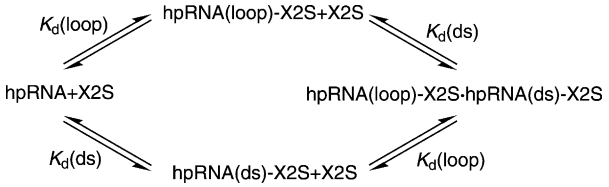

complexes of X2S derivatives with hpRNA at the double-stranded and loop regions, respectively. Subscript t indicates the total amount. For the fitting of K_d(loop) in Equation (2), we used the K_d(ds) value obtained from the titration with dsRNA by Equation (1). K_d(loop) [M] was obtained with an R^2 value higher than 0.88 and was 5.2×10^{-8} for **3a**, 1.3×10^{-8} for **3b**, 1.7×10^{-8} for **3c**, 3.7×10^{-7} for **3d**, and 1.1×10^{-6} for **3e**. The curve-fitted plots and R^2 values are shown in Figure 5. The analysis suggested that the affinity to the double-stranded region increased upon increasing the linker length, whereas the affinity to the loop region decreased by a factor of 20. The affinity of **3d** and **3e** to dsRNA was similar to that to hpRNA, whereas the affinity of **3e** to dsRNA was about 30 times stronger than that to hpRNA. The electrostatic association of two positively charged ammonium groups to the negatively charged phosphate anions may rationalize the higher affinity of the X2S derivative with a long alkyl chain. It is reasonable to assume that as the distance between the two ammonium groups becomes longer, the probability of simultaneous electrostatic interactions of the two charged ammonium groups with the negatively charged phosphate would be higher.

$$\frac{F}{F_0}=\frac{-a+2\sqrt{a^2-3b}}{3[\mathrm{X2S}]_t}\cos\left(\arccos\frac{-2a^3+9ab-27c}{6\sqrt{(a^2-3b)^3}}\right)$$
$$a=K_d(\mathrm{ds})+K_d(\mathrm{loop})+2[\mathrm{RNA}]_t-[\mathrm{X2S}]_t$$
$$b=\{[\mathrm{RNA}]_t-[\mathrm{X2S}]_t\}\{K_d(\mathrm{ds})+K_d(\mathrm{loop})\}+K_d(\mathrm{ds})K_d(\mathrm{loop})$$
$$c=-K_d(\mathrm{ds})K_d(\mathrm{loop})[\mathrm{X2S}]_t \quad (2)$$

The effect of the methyl substituent at the side chain on the fluorescence quenching was not apparent for dsRNA, but was marked for hpRNA (Figure 6). Three methyl-substituted X2S derivatives **3f**, **3g**, and **4** showed similar plots when titrated with dsRNA. The lowest efficiency in fluorescence quenching by dsRNA was observed for the *N*,*N*-dimethyl derivative **4**. Both **3f** and **3g** with a methyl substituent on the linker at the C1′ and C2′ position, respectively, showed a similar plot to that obtained for **3a**. In marked contrast, the titration plot of **3f** obtained with hpRNA was not much different from that obtained with dsRNA, whereas derivatives **3g** and **4** showed fluorescence quenching in

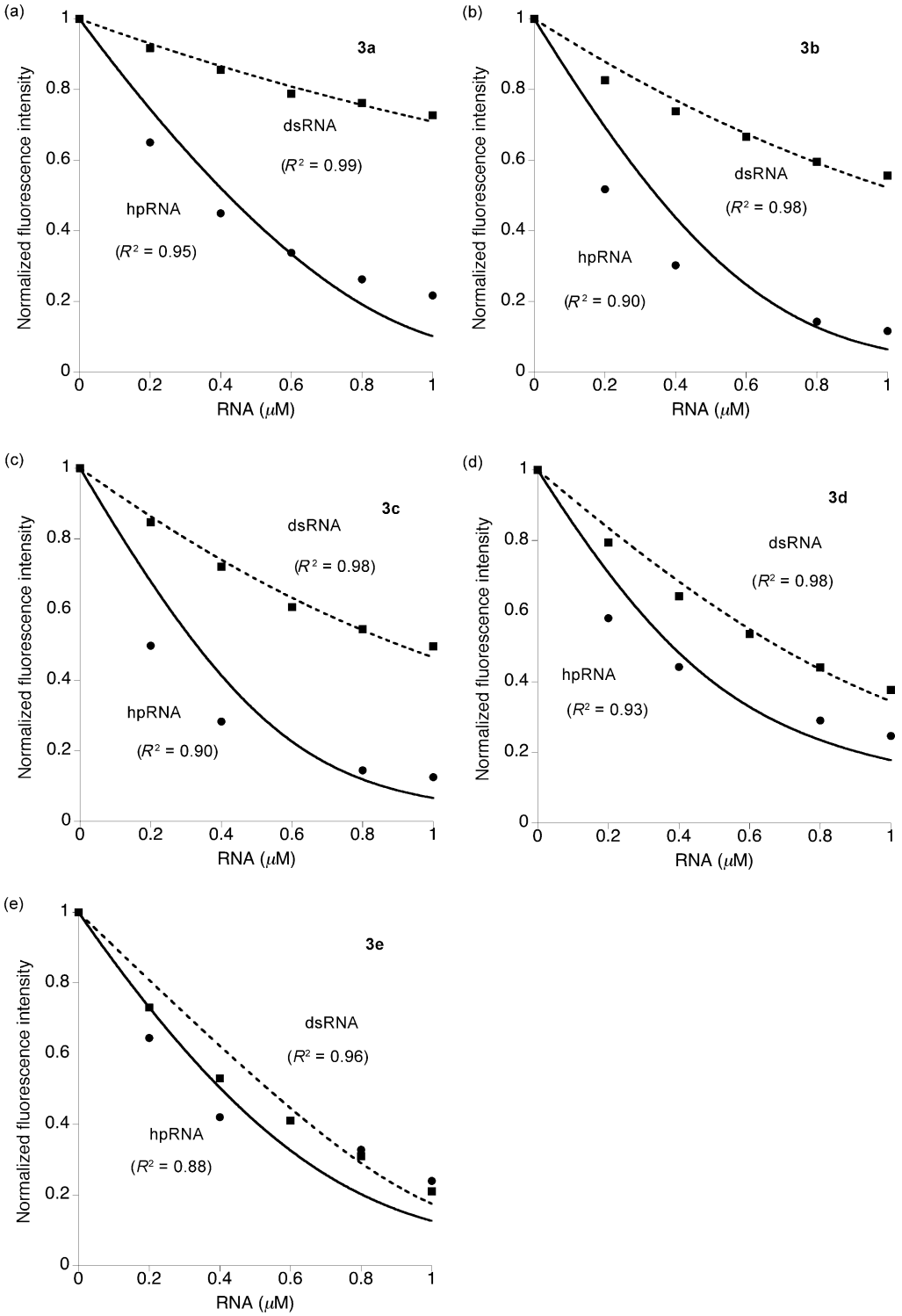

Figure 5. a–e) Relative fluorescence intensity of xanthone derivatives **3a–e** (1 μM), respectively, titrated with various concentrations of dsRNA (■) and hpRNA (●). Dotted and solid lines represent nonlinear least-squares-fitted curves derived by fitting the data with Equations (1) and (2), respectively. The coefficient of determination R^2 is shown in the graphs and summarized in Table 2.

a concentration-dependent manner with a reduced efficiency compared to **3a**. This suggested that the methyl group at the C1′ position effectively hindered the binding of **3f** to the loop region of hpRNA.

The curve fitting analysis of the titration data for **3f**, **3g**, and **4** with Equation (1) was successfully carried out, with the coefficient of determination being higher than 0.93 (Figure 6), and showed that the affinity of **4** to the dsRNA

Table 2. Apparent dissociation constants K_d [M] of the complex of each indicator and double-stranded region and loop region of RNA.

	3a	3b	3c	3d	3e	3f	3g	4
K_d(ds)	1.7×10^{-6}	5.7×10^{-7}	4.0×10^{-7}	1.8×10^{-7}	3.7×10^{-8}	1.6×10^{-6}	1.2×10^{-6}	4.3×10^{-6}
R^2[a]	(0.99)	(0.98)	(0.98)	(0.98)	(0.96)	(0.93)	(1.0)	(0.97)
K_d(loop)	5.2×10^{-8}	1.3×10^{-8}	1.7×10^{-8}	3.7×10^{-7}	1.1×10^{-6}	2.8×10^{-6}	2.0×10^{-7}	1.7×10^{-7}
R^2[a]	(0.95)	(0.90)	(0.90)	(0.93)	(0.88)	(0.95)	(0.96)	(0.97)
relK_d(ds)[b]	1	3.0	4.3	9.5	46	1.1	1.4	0.4
relK_d(loop)	1	4.0	3.1	0.14	0.05	0.02	0.26	0.31
SI[c]	33	45	23	0.5	0.03	0.6	6	25

[a] R^2 represents the coefficient of determination obtained for nonlinear least-squares fitting. [b] relK_d(ds) = [K_d(ds) of **3a**]/K_d(ds). [c] SI (selectivity index) = K_d(ds)/K_d(loop).

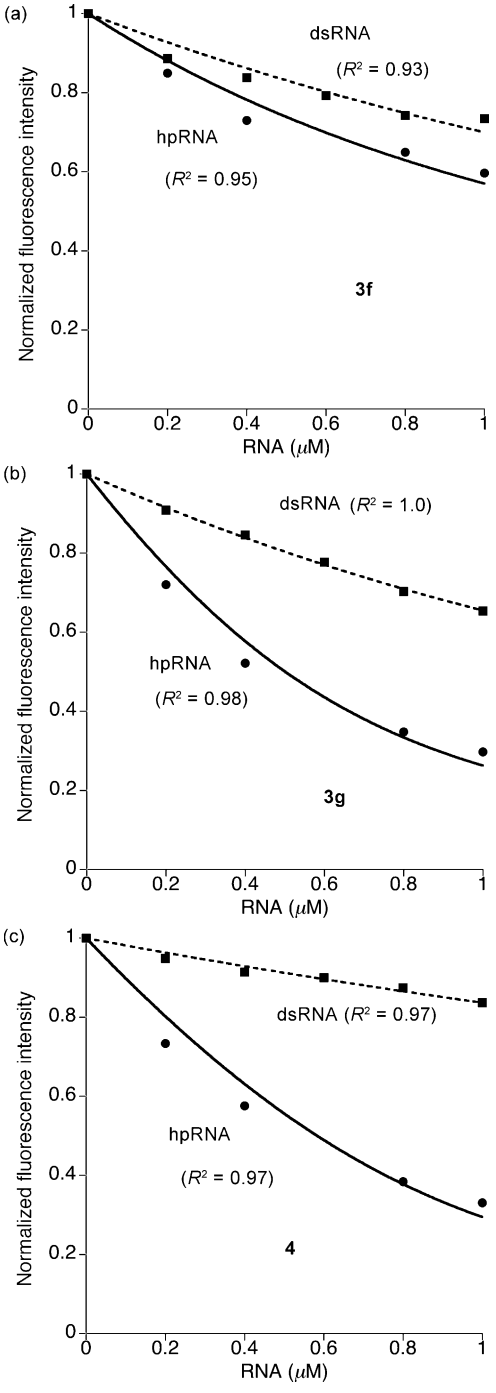

Figure 6. Relative fluorescence intensity of xanthone derivatives a) **3f**, b) **3g**, and c) **4** (1 μM) with various concentrations of dsRNA (■) and hpRNA (●). Dotted and solid lines represent nonlinear least-squares-fitted curves derived by fitting the data with Equations (1) and (2), respectively. The coefficient of determination R^2 is shown in the graphs and summarized in Table 2.

was 2.5 times weaker than the affinity of the parent molecule **3a**, which showed the lowest affinity to dsRNA among the molecules discussed in these studies. The apparent dissociation constant of the complex of methyl-substituted X2S derivative at the loop region of hpRNA was obtained by curve fitting analysis using Equation (2), with the R^2 value being higher than 0.95. The affinity of **3f** to the loop region of hpRNA (2.8×10^{-6} M) was almost comparable to that to dsRNA (1.6×10^{-6} M), whereas the affinity of **3g** and **4** to the loop region of hpRNA was 2.0×10^{-7} and 1.7×10^{-7} M, respectively, and was 6 and 26 times stronger than that to dsRNA (Table 2). The remarkable effect of methyl substitution at the C1′ position in **3f** is most likely ascribable to the steric hindrance of the methyl group. Conformational analyses of **3f** suggested that the methyl group of **3f** in low-energy conformers favors the position perpendicular to the xanthone plane, thus making it less susceptible to intercalative binding into the base pairs in the stem loop regions.

The binding characteristics of fluorescent indicators were assessed by K_d(ds), K_d(loop), and the selectivity index (SI), which was calculated by the ratio of two dissociation constants (K_d(ds)/K_d(loop)). The affinities of each compound to the double-stranded and loop regions were also compared with the affinities of the parent compound **3a**. Thus, relative K_d(ds) [relK_d(ds)] and K_d(loop) [relK_d(loop)] values were calculated by dividing the K_d of **3a** by the K_d of each compound. The relK_d(ds) values clearly showed that the *N*,*N*-dimethyl derivative **4** is the only compound showing a weaker affinity to dsRNA than the parent compound **3a**. The relK_d(loop) was significantly affected by the linker structure. Compounds **3b** and **3c** showed higher affinity to the loop region than **3a**, whereas compound **4** still retained about one third of the affinity of **3a** to the loop region. The selectivity index of the affinity to the loop region over the double-stranded region decreased in the order of **3b**, **3a**, **4**, and **3c**.

The thioxanthone derivative **5** and its *N*,*N*-dimethyl derivative **6** showed a similar quenching profile to **3a** when titrated with dsRNA (Figure 7). The affinity to dsRNA was calculated to be 8.3×10^{-7} (R^2 = 0.97) for **5** and 1.5×10^{-6} (R^2 = 0.89) for **6**. Fluorescence quenching by hpRNA was more efficient for both **5** and **6** than for **3a**. The titration data for **5** and **6** with hpRNA, however, did not fit well to Equa-

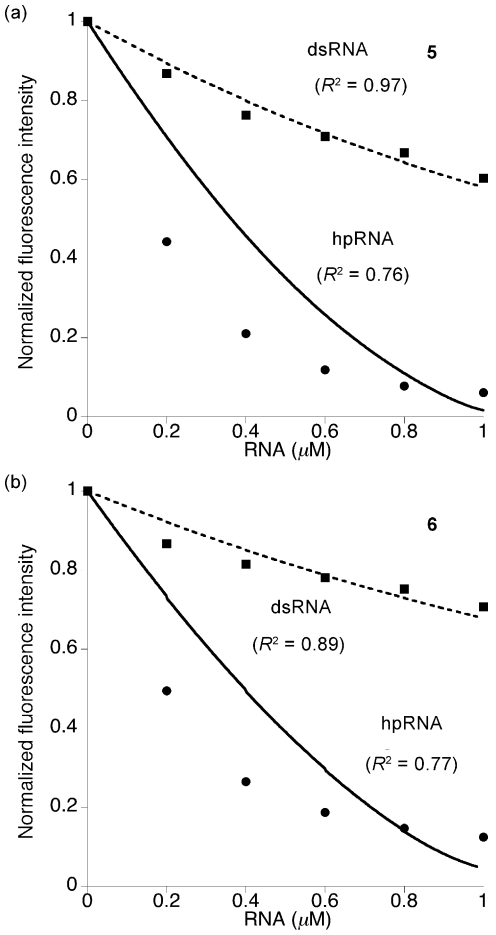

Figure 7. Relative fluorescence intensity of xanthone derivatives a) **5** and b) **6** (1 μM) with various concentrations of dsRNA (■) and hpRNA (●). Dotted and solid lines represent nonlinear least-squares-fitted curves derived by fitting the data with Equations (1) and (2), respectively. The coefficient of determination R^2 is shown in the graphs and summarized in Table 2.

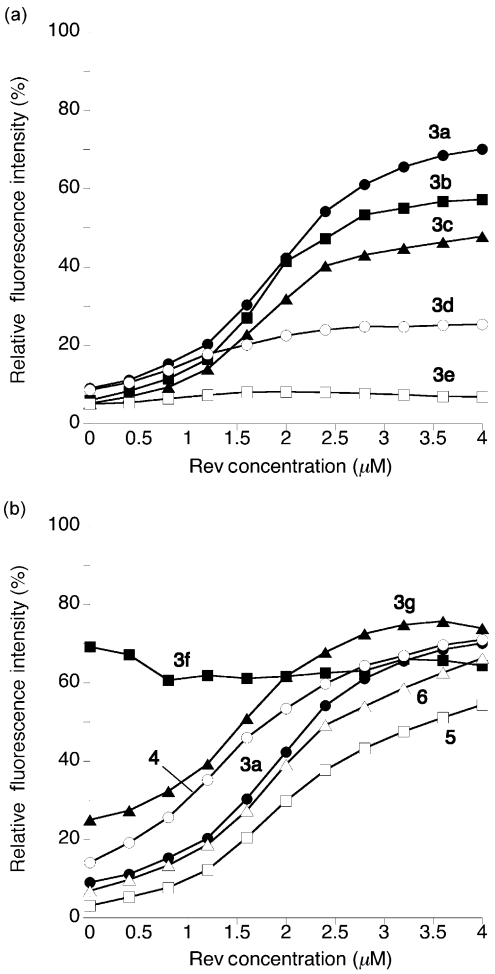

Figure 8. Recovered fluorescence intensity of xanthone and thioxanthone derivatives upon titrating the indicator–hpRNA complex (each 2 μM) with Rev peptide. Solid lines are provided as a guide to the eye.

tion (2). The coefficient of determination obtained for the curve fitting was 0.76 for **5** and 0.77 for **6** with an unreasonable K_d(loop) of 6.0×10^{-10} and 4.4×10^{-9}, respectively. The slope of the profile of fluorescence quenching for **5** and **6** was much steeper than that for **3a**, thus suggesting that thioxanthone derivatives are more prominent than xanthone derivatives for multiple binding to the loop region.

Displacement with Rev peptide: Fluorimetric titration experiments with dsRNA and hpRNA revealed that synthetic xanthone and thioxanthone derivatives showed diverse affinity to the dsRNA and hpRNA depending on the length and structures of the linker as well as the chromophore. We then examined the displacement of the bound indicators to hpRNA by the titration of Rev peptide (Figure 8). We expected an increase of the fluorescence intensity of the indicator upon displacement of the bound indicator with Rev peptide. First, we examined the displacement of xanthone derivatives with a different linker length. As shown in Figure 8a, the profile of fluorescence recovery was indicator-dependent. A sigmoidal profile of fluorescence recovery was observed for **3a** as we reported earlier, the fluorescence intensity at saturation gradually decreasing with increasing linker length. With **3e**, which has the longest linker length and the highest affinity to dsRNA, we did not observe any fluorescence recovery even at a Rev peptide concentration of 4 μM. This is most likely ascribable to the increased affinity of xanthone derivatives to the dsRNA with concomitant decreased affinity to the hpRNA. As anticipated from the weak affinity of **3f** to both dsRNA and hpRNA, the fluorescence intensity of **3f** in the presence of hpRNA did not change upon titration with Rev peptide (Figure 8b). Other xanthone and thioxanthone derivatives showed similar fluorescence recovery to that of **3a** with different fluorescence intensity at saturation with a Rev peptide concentration of 4 μM.

Conclusion

Structurally modified derivatives of **3a** were synthesized and their spectroscopic and RNA-binding properties were investigated. The *N*,*N*-dimethyl derivative **4** showed a lower affinity to the double-stranded region than the parent **3a** by compensating for the decrease of the affinity to the loop region by one third. From the viewpoint of fluorescent indicators for FID, we concluded that the *N*,*N*-dimethyl derivative **4** would be the choice for screening RRE-binding molecules. Thioxanthone derivatives have intrinsic advantages over xanthones in terms of their longer excitation wavelength. The *N*,*N*-dimethyl derivative **6** is also useful for the FID assay, but it is important to note that the thioxanthone derivatives tend to bind to RNA with multiple stoichiometry.

The marked effect of the linker length and structures tethering amino groups on the affinity to RNA suggested the potential of the auxiliary functional groups and structures for modulating the affinity of the indicator to specific RNA structures. In particular, the substituents on the amino groups having diverse structures and providing hydrogen-bonding, electrostatic, and hydrophobic interactions to the nucleotide bases and sugar–phosphate backbone may provide an important class of compounds, not only for the indicator in FID but also for potential lead compounds of RNA-binding molecules.

Experimental Section

General: Reagents and solvents were purchased from standard suppliers and used without further purification. Reactions were monitored with TLC plates precoated with Merck silica gel 60 F_{254}. Spots were visualized with UV light or ninhydrin. ^{1}H and ^{13}C NMR spectra were recorded with JEOL JNM-LA400 and LA600 instruments. The chemical shifts are expressed in ppm relative to residual solvent as an internal standard. ESI mass spectra were recorded on a JEOL AccuTOF JMS-T100N mass spectrometer. Absorption spectra were recorded with a Beckman Coulter DU800 UV/Vis spectrophotometer, and fluorescence with a Shimazdu RF-5300PC spectrometer. Quantum yields were recorded with a PL Quantum Yield Measurement System 9920-02 (Hamamatsu Photonics).

2,7-Bis(*N*-Boc-2-aminoethoxy)xanthone (2a): 2,7-Dihydroxyxanthone (**1**)[14] (92.0 mg, 0.403 mmol) and triphenylphosphine (271 mg, 1.03 mmol) were dried by their azeotrope with toluene, and dissolved in dry THF (2.5 mL) under an argon atmosphere. Diethyl azodicarboxylate (460 μL, 40% in toluene, 1.01 mol) was added to the solution at room temperature, and then *N*-Boc-aminoethanol (158 mg, 0.949 mmol) was added dropwise. The reaction mixture was stirred at room temperature overnight, and then at 55 °C for 5 h. The solvent was evaporated and the residue was purified by column chromatography on silica gel with elution by chloroform and ethyl acetate (100:1 to 100:5). The product was further purified by gel permeation chromatography to give **2a** (110 mg, 53%) as a white solid. ^{1}H NMR (400 MHz, $CDCl_3$): δ = 1.46 (s, 18H), 3.59 (m, 4H), 4.14 (t, J = 5.1 Hz, 4H), 5.00 (broad, 2H), 7.33 (dd, J = 3.0, 9.3 Hz, 2H), 7.45 (d, J = 9.0 Hz, 2H), 7.68 ppm (d, J = 2.9 Hz, 2H); ^{13}C NMR (150 MHz, $CDCl_3$): δ = 28.89, 29.69, 40.00, 67.88, 106.84, 119.49, 121.47, 124.82, 151.10, 154.80, 155.82, 176.72 ppm; HRMS (ESI): m/z calcd for $C_{27}H_{34}N_2NaO_8$: 537.2213 $[M+Na]^+$; found: 537.2189.

2,7-Bis(2-aminoethoxy)xanthone (3a): 2,7-Bis(*N*-Boc-2-aminoethoxy)-xanthone (**2a**; 43.7 mg, 85 μmol) was added to 4N HCl in EtOAc (5.0 mL) and stirred at room temperature for 4 h, giving a white precipitate. The solvent was evaporated, the residue was dissolved in water, and the solution was filtered and lyophilized, to give **3a** as a white solid. ^{1}H NMR (600 MHz, D_2O): δ = 3.48 (t, J = 4.8 Hz, 4H), 4.29 (t, J = 4.8 Hz, 4H), 7.36 (d, J = 3.0 Hz, 2H), 7.39–7.43 ppm (4H); HRMS (ESI): m/z calcd for $C_{17}H_{19}N_2O_4$: 315.1345 $[M+H]^+$; found: 315.1334.

2,7-Bis(*N*-Boc-3-aminopropoxy)xanthone (2b): ^{1}H NMR (600 MHz, $CDCl_3$): δ = 1.45 (s, 18H), 2.04 (quintet, J = 5.5 Hz, 4H), 3.37 (m, 4H), 4.15 (t, J = 5.9 Hz, 4H), 4.74 (broad, 2H), 7.33 (dd, J = 3.3, 9.1 Hz, 2H), 7.44 (d, J = 9.1 Hz, 2H), 7.69 ppm (d, J = 2.9 Hz, 2H); ^{13}C NMR (100 MHz, $CDCl_3$): δ = 28.38, 29.44, 37.89, 66.35, 79.26, 106.43, 119.37, 121.40, 125.00, 150.96, 155.01, 155.97, 176.79 ppm; HRMS (ESI): m/z calcd for $C_{29}H_{38}N_2NaO_8$: 565.2526 $[M+Na]^+$; found: 565.2526.

2,7-Bis(3-aminopropoxy)xanthone (3b): ^{1}H NMR (600 MHz, D_2O): δ = 2.20 (quintet, J = 6.6 Hz, 4H), 3.24 (t, J = 6.6 Hz, 4H), 4.11 (t, J = 5.4 Hz, 4H), 7.21 (broad, 2H), 7.28–7.33 ppm (4H); HRMS (ESI): m/z calcd for $C_{19}H_{23}N_2O_4$: 343.1658 $[M+H]^+$; found: 343.1645.

2,7-Bis(*N*-Boc-4-aminobutoxy)xanthone (2c): ^{1}H NMR (400 MHz, $CDCl_3$): δ = 1.45 (s, 18H), 1.71 (quintet, J = 7.3 Hz, 4H), 1.87 (quintet, J = 6.2 Hz, 4H), 3.22 (m, 4H), 4.10 (t, J = 6.2 Hz, 4H), 4.63 (broad, 2H), 7.32 (dd, J = 2.9, 9.2 Hz, 2H), 7.43 (d, J = 9.1 Hz, 2H), 7.67 ppm (d, J = 2.9 Hz, 2H); ^{13}C NMR (100 MHz, $CDCl_3$): δ = 26.48, 26.84, 28.39, 40.28, 68.21, 79.13, 106.37, 119.32, 121.40, 125.00, 150.89, 155.11, 155.97, 176.86 ppm; HRMS (ESI): m/z calcd for $C_{31}H_{42}N_2NaO_8$: 593.2839 $[M+Na]^+$; found: 593.2839.

2,7-Bis(4-aminobutoxy)xanthone (3c): ^{1}H NMR (600 MHz, D_2O): δ = 1.82–1.90 (8H), 3.09 (t, J = 7.2 Hz, 4H), 3.98 (t, J = 5.1 Hz, 4H), 7.09 (broad, 2H), 7.18–7.26 ppm (4H); HRMS (ESI): m/z calcd for $C_{21}H_{27}N_2O_4$: 371.1971 $[M+H]^+$; found: 371.1959; m/z calcd for $C_{21}H_{26}N_2NaO_4$: 393.1790 $[M+Na]^+$; found: 393.1778.

2,7-Bis(*N*-Boc-5-aminopentanoxy)xanthone (2d): ^{1}H NMR (600 MHz, $CDCl_3$): δ = 1.44 (s, 18H), 1.48–1.60 (8H), 1.84 (quintet, J = 7.6 Hz, 4H), 3.16 (m, 4H), 4.06 (t, J = 6.2 Hz, 4H), 4.58 (broad, 2H), 7.30 (dd, J = 2.8, 8.9 Hz, 2H), 7.41 (d, J = 8.9 Hz, 2H), 7.66 ppm (d, J = 2.8 Hz, 2H); ^{13}C NMR (100 MHz, $CDCl_3$): δ = 23.34, 28.40, 28.80, 29.84, 40.44, 68.40, 79.06, 106.31, 119.30, 121.42, 125.05, 150.86, 155.23, 155.97, 176.90 ppm; HRMS (ESI): m/z calcd for $C_{33}H_{46}N_2NaO_8$: 621.3152 $[M+Na]^+$; found: 621.3151.

2,7-Bis(5-aminopentanoxy)xanthone (3d): ^{1}H NMR (600 MHz, $CDCl_3$): δ = 1.51 (quintet, J = 7.8 Hz, 4H), 1.75 (quintet, J = 7.8 Hz, 4H), 1.79 (quintet, J = 7.8 Hz, 4H), 3.03 (t, J = 7.8 Hz, 4H), 3.86 (t, J = 6.3 Hz, 4H), 6.92 (d, J = 2.4 Hz, 2H), 7.07 (dd, J = 3.3, 9.3 Hz, 2H), 7.13 ppm (d, J = 9.0 Hz, 2H); HRMS (ESI): m/z calcd for $C_{23}H_{31}N_2O_4$: 399.2284 $[M+H]^+$; found: 399.2272; m/z calcd for $C_{23}H_{30}N_2NaO_4$: 421.2103 $[M+Na]^+$; found: 421.2090.

2,7-Bis(*N*-Boc-6-aminohexanoxy)xanthone (2e): ^{1}H NMR (600 MHz, $CDCl_3$): δ = 1.44 (s, 18H), 1.38–1.55 (12H), 1.83 (quintet, J = 7.6 Hz, 4H), 3.14 (m, 4H), 4.07 (t, J = 6.5 Hz, 4H), 4.54 (broad, 2H), 7.31 (dd, J = 3.4, 8.9 Hz, 2H), 7.42 (d, J = 8.9 Hz, 2H), 7.67 ppm (d, J = 3.4 Hz, 2H); ^{13}C NMR (100 MHz, $CDCl_3$): δ = 25.76, 26.55, 28.41, 29.06, 30.02, 40.51, 68.53, 79.02, 106.35, 119.29, 121.44, 125.06, 150.86, 155.29, 155.98, 176.93 ppm; HRMS (ESI): m/z calcd for $C_{35}H_{50}N_2NaO_8$: 649.3465 $[M+Na]^+$; found: 649.3467.

2,7-Bis(6-aminohexanoxy)xanthone (3e): ^{1}H NMR (400 MHz, D_2O): δ = 1.49–1.53 (8H), 1.72–1.82 (8H), 3.06 (t, J = 7.6 Hz, 4H), 3.85 (t, J = 6.4 Hz, 4H), 6.89 (d, J = 2.8 Hz, 2H), 4.58 (broad, 2H), 7.30 (dd, J = 2.8, 8.9 Hz, 2H), 7.05 (dd, J = 2.8, 9.2 Hz, 2H), 7.12 ppm (d, J = 9.2 Hz, 2H); HRMS (ESI): m/z calcd for $C_{25}H_{35}N_2O_4$: 427.2597 $[M+H]^+$; found: 427.2580; m/z calcd for $C_{25}H_{34}N_2NaO_4$: 449.2416 $[M+Na]^+$; found: 449.2399.

2,7-Bis(1-*N*-Boc-amino-2-propoxy)xanthone (2f): The two diastereomers could not be separated, therefore, we report the NMR data for the mixture. ^{1}H NMR (600 MHz, $CDCl_3$): δ = 1.33 (d, J = 6.6 Hz, 6H), 1.44 (s, 18H), 3.30 (2H), 3.53 (2H), 4.54 (2H), 4.94 (broad, 2H), 7.31 (dd, J = 2.7, 8.7 Hz, 2H), 7.43 (d, J = 9.0 Hz, 2H), 7.72 ppm (d, J = 2.4 Hz, 2H); ^{13}C NMR (100 MHz, $CDCl_3$): δ = 16.81, 28.36, 45.45, 74.05, 79.51, 108.90, 119.48, 121.53, 125.74, 150.98, 153.73, 155.96, 176.64 ppm; HRMS (ESI): m/z calcd for $C_{29}H_{38}N_2NaO_8$: 565.2526 $[M+Na]^+$; found: 565.2519.

2,7-Bis(1-amino-2-propoxy)xanthone (3f): ^{1}H NMR (400 MHz, D_2O): δ = 1.44–1.46 (6H), 3.26–3.33 (2H), 3.38–3.44 (2H), 4.80–4.85 (2H), 7.38–7.48 (4H), 7.49–7.51 ppm (2H); HRMS (ESI): *m*/*z* calcd for $C_{19}H_{23}N_2O_4$: 343.1658 $[M+H]^+$; found: 343.1649; *m*/*z* calcd for $C_{19}H_{22}N_2NaO_4$: 365.1477 $[M+Na]^+$; found: 365.1468.

2,7-Bis(*N*-Boc-2-aminopropoxy)xanthone (2g): The two diastereomers could not be separated, therefore, we report the NMR data for the mixture. ^{1}H NMR (600 MHz, $CDCl_3$): δ = 1.32 (d, *J* = 6.9 Hz, 6H), 1.46 (s, 18H), 4.03 (d, *J* = 3.4 Hz, 4H), 4.11 (m, 2H), 4.79 (broad, 2H), 7.33 (dd, *J* = 2.8, 8.9 Hz, 2H), 7.42 (d, *J* = 8.9 Hz, 2H), 7.66 ppm (d, *J* = 2.8 Hz, 2H); ^{13}C NMR (100 MHz, $CDCl_3$): δ = 17.93, 28.38, 45.82, 71.73, 79.50, 106.82, 119.38, 121.42, 124.82, 151.03, 154.96, 155.22, 176.69 ppm; HRMS: *m*/*z* calcd for $C_{29}H_{38}N_2NaO_8$: 565.2526 $[M+Na]^+$; found: 565.2520.

2,7-Bis(2-aminopropoxy)xanthone (3g): ^{1}H NMR (400 MHz, D_2O): δ = 1.47–1.49 (6H), 3.80–3.90 (2H), 4.05–4.15 (2H), 4.20–4.30 (2H), 7.30–7.50 ppm (6H); HRMS (ESI): *m*/*z* calcd for $C_{19}H_{23}N_2O_4$: 343.1658 $[M+H]^+$; found: 343.1648; *m*/*z* calcd for $C_{19}H_{22}N_2NaO_4$: 365.1477 $[M+Na]^+$; found: 365.1467.

2,7-Bis[2-(*N*,*N*-dimethylamino)ethoxy]xanthone (4): ^{1}H NMR (600 MHz, CD_3OD): δ = 2.39 (s, 12H), 2.85 (t, *J* = 5.3 Hz, 4H), 4.22 (t, *J* = 5.3 Hz, 4H), 7.45 (dd, *J* = 2.9, 9.2 Hz, 2H), 7.53 (d, *J* = 9.2 Hz, 2H), 7.66 ppm (d, *J* = 2.9 Hz, 2H); ^{13}C NMR (100 MHz, CD_3OD): δ = 45.80, 58.95, 67.17, 107.35, 120.81, 122.31, 126.45, 152.49, 156.54, 178.38 ppm; HRMS: *m*/*z* calcd for $C_{21}H_{27}N_2NaO_4$: 371.1971 $[M+Na]^+$; found: 371.1965.

2,7-Dihydroxythioxanthone: 2,7-Dimethoxythioxanthone[15] (500 mg, 1.84 mmol) was dissolved in dichloromethane (8 mL) under an argon atmosphere. The reaction mixture was cooled at 0 °C and BBr_3 (18 mL, 1.0 mol L^{-1} in dichloromethane, 18 mmol) was added carefully. The temperature was allowed to rise to room temperature and the mixture was stirred overnight. The reaction mixture was cooled at 0 °C and ice was added carefully to quench the reaction. The reaction mixture was extracted with ethyl acetate and dried over magnesium sulfate. The solvent was evaporated and the residue was purified by column chromatography employing hexane and ethyl acetate (2:1 to 1:1) to give 2,7-dihydroxythioxanthone as a yellow powder (363 mg, 81%). ^{1}H NMR (600 MHz, [D_6]DMSO): δ = 7.23 (dd, *J* = 2.8, 8.8 Hz, 2H), 7.64 (d, *J* = 8.8 Hz, 2H), 7.82 ppm (d, *J* = 2.8 Hz, 2H); ^{13}C NMR (150 MHz, [D_6]DMSO): δ = 113.09, 122.60, 126.75, 127.96, 129.03, 156.18, 178.40 ppm; HRMS (ESI): *m*/*z* calcd for $C_{13}H_8NaO_3S$: 267.0092 $[M+Na]^+$; found: 267.0079.

2,7-Bis(*N*-Boc-2-aminoethoxy)thioxanthone: ^{1}H NMR (600 MHz, $CDCl_3$): δ = 1.46 (s, 18H), 3.54–3.62 (4H), 4.15 (t, *J* = 5.4 Hz, 4H), 5.00 (broad, 2H), 7.24 (dd, *J* = 3.3, 8.7 Hz, 2H), 7.50 (d, *J* = 9.0 Hz, 2H), 8.03 ppm (d, *J* = 1.8 Hz, 2H); ^{13}C NMR (150 MHz, $CDCl_3$): δ = 28.55, 40.13, 67.78, 79.79, 111.52, 121.47, 122.71, 127.57, 129.73 129.89, 155.99, 157.37, 179.32 ppm; HRMS (ESI): *m*/*z* calcd for $C_{27}H_{34}N_2NaO_7S$: 553.1984 $[M+Na]^+$; found: 553.1960.

2,7-Bis(2-aminoethoxy)thioxanthone (5): ^{1}H NMR (400 MHz, D_2O): δ = 3.48 (t, *J* = 4.8 Hz, 4H), 4.29 (t, *J* = 4.8 Hz, 4H), 7.25 (dd, *J* = 2.8, 8.8 Hz, 2H), 7.50 (d, *J* = 9.2 Hz, 2H), 7.64 ppm (d, *J* = 2.8 Hz, 2H); HRMS (ESI): *m*/*z* calcd for $C_{17}H_{19}N_2O_3S$: 331.1116 $[M+H]^+$; found: 331.1102.

2,7-Bis[2-(*N*,*N*-dimethylamino)ethoxy]xanthone (6): ^{1}H NMR (600 MHz, CD_3OD): δ = 2.98 (s, 12H), 3.62 (t, *J* = 5.1 Hz, 4H), 4.51 (t, *J* = 4.8 Hz, 4H), 7.51 (dd, *J* = 2.7, 8.7 Hz, 2H), 7.76 (d, *J* = 9.0 Hz, 2H), 8.16 ppm (d, *J* = 3.6 Hz, 2H); ^{13}C NMR (150 MHz, $CDCl_3$): 45.94, 58.30, 66.24, 110.97, 127.46, 129.65, 129.74, 157.64, 179.51 ppm; HRMS (ESI): *m*/*z* calcd for $C_{21}H_{27}N_2O_3S$: 387.1742 $[M+H]^+$; found: 387.1731.

Spectroscopic measurements: The UV spectra of xanthone derivatives (100 μM) were recorded in sodium cacodylate buffer (10 mM, pH 7.0) containing NaCl (100 mM). Quantum yields were recorded with xanthone and thioxanthone derivatives (20–50 μM), the concentration showing adequate absorption of photons. The fluorescence spectra of xanthone derivatives (2 μM) were recorded in sodium cacodylate buffer (10 mM, pH7) containing NaCl (100 mM).

Nonlinear least-squares fitting of fluorescence titration data: All curve fitting was carried out by using SigmaPlot 2001. The data obtained during titration of indicators with dsRNA were fitted to Equation (1), assuming a 1:1 binding model, to give the K_d(ds) value. The data obtained during titration of indicators with hpRNA were fitted to Equation (2), assuming two independent binding site models. To calculate K_d(loop), we employed the K_d(ds) value derived from fitting of the titration data with dsRNA.

Fluorimetric titration with RNA: All titrations were performed with a working solution of each indicator (1.0 μM) in sodium cacodylate buffer (10 mM, pH 7.0) containing NaCl (100 mM). During titration, the indicator was excited at its excitation maximum, and the changes in emission were monitored at the emission maximum of the indicators. Relative fluorescence intensity is the percentage of fluorescence intensity observed in each measurement relative to that of free indicator. The values relK_d were calculated by dividing the K_d value of **3a** by the K_d value of each indicator as an index to compare the affinity of indicators. The selectivity to the loop region was estimated by the selectivity index (SI) obtained by dividing the K_d(ds) value by the K_d(loop) value of the indicator.

Displacement assay: A solution of each indicator (2.0 μM) mixed with hpRNA (2.0 μM) in sodium cacodylate buffer (10 mM, pH 7.0) containing NaCl (100 mM) was titrated with Rev peptide. Changes in the fluorescence intensity during the titration were monitored at the emission maximum.

Acknowledgements

This work was supported by the Uehara Memorial Foundation, a Grant-in-Aid for Scientific Research (A; 11000432) from JSPS, and the Program for Promotion of Fundamental Studies in Health Sciences of the National Institute of Biomedical Innovation (NIBIO, 10-22). We thank Prof. Takashi Morii and Dr. Masatora Fukuda of Kyoto University for the generous gift of Rev peptide, and Prof. Kazuo Harada of Tokyo Gagugei University for valuable discussions. S.U. is grateful for the support by JSPS Fellows (21, 1350).

[1] a) S. L. Wiskur, H. Ait-Haddou, J. J. Lavigne, E. V. Anslyn, *Acc. Chem. Res.* **2001**, *34*, 963–972; b) B. T. Nguyen, E. V. Anslyn, *Coord. Chem. Rev.* **2006**, *250*, 3118–3127; c) L. Zhu, E. V. Anslyn, *J. Am. Chem. Soc.* **2004**, *126*, 3676–3677; d) B. T. Nguyen, S. L. Wiskur, E. V. Anslyn, *Org. Lett.* **2004**, *6*, 2499–2501.

[2] a) W. C. Tse, D. L. Boger, *Acc. Chem. Res.* **2004**, *37*, 61–69; b) D. L. Boger, B. E. Fink, S. R. Brunette, W. C. Tse, M. P. Hedrick, *J. Am. Chem. Soc.* **2001**, *123*, 5878–5891; c) D. L. Boger, B. E. Fink, M. P. Hedrick, *J. Am. Chem. Soc.* **2000**, *122*, 6382–6394.

[3] a) Y. Wang, R. R. Rando, *Chem. Biol.* **1995**, *2*, 281–290; b) K. Hamasaki, R. R. Rando, *Anal. Biochem.* **1998**, *261*, 183–190; c) K. D. Goodwin, M. A. Lewis, F. A. Tanious, R. R. Tidwell, W. D. Wilson, M. M. Georgiadis, E. C. Long, *J. Am. Chem. Soc.* **2006**, *128*, 7846–7854; d) D. Monchaud, C. Allain, H. Bertrand, N. Smargiasso, F. Rosu, V. Gabelica, A. De Cian, J.-L. Mergny, M.-P. Teulade-Fichou, *Biochimie* **2008**, *90*, 1207–1223; e) M. Krishnamurthy, N. T. Schirle, P. A. Beal, *Bioorg. Med. Chem.* **2008**, *16*, 8914–8921; f) P. N. Asare-Okai, C. S. Chow, *Anal. Biochem.* **2011**, *408*, 269–276.

[4] For FID studies with covalent modification, see: a) N. W. Luedtke, Y. Tor, *Biopolymers* **2003**, *70*, 103–199; b) K. J. Blount, Y. Tor, *Nucleic Acids Res.* **2003**, *31*, 5490–5500; c) T. D. Bradrick, J. P. Marino, *RNA* **2004**, *10*, 1459–1468; d) Z. Yan, A. M. Baranger, *Bioorg. Med. Chem. Lett.* **2004**, *14*, 5889–5893; e) R. Kawai, M. Kimoto, S. Ikeda, T. Mitsui, M. Endo, S. Yokoyama, I. Hirao, *J. Am. Chem. Soc.* **2005**, *127*, 17286–17295; f) M. Hagihara, M. Fukuda, T. Hasegawa, T. Morii, *J. Am. Chem. Soc.* **2006**, *128*, 12932–12940; g) K. Lang, R. Rieder, R. Micura, *Nucl. Acids Res.* **2007**, *35*, 5370–5378; h) Y. Xie, A. V. Dix, Y. Tor, *J. Am. Chem. Soc.* **2009**, *131*, 17605–17614; i) H. S. Jeong, S. Kang, J. Y. Lee, B. H. Kim, *Org. Biomol. Chem.* **2009**, *7*, 921–925; j) Y. Xie, T. Maxson, Y. Tor, *J. Am. Chem. Soc.* **2010**, *132*, 11896–11897.

[5] J. Zhang, S. Umemoto, K. Nakatani, *J. Am. Chem. Soc.* **2010**, *132*, 3660–3661.
[6] a) C. S. Chow, F. M. Bogdan, *Chem. Rev.* **1997**, *97*, 1489–1514; b) N. D. Pearson, C. D. Prescott, *Chem. Biol.* **1997**, *4*, 409–414; c) T. Hermann, E. Westhof, *Curr. Opin. Biotechnol.* **1998**, *9*, 66–73; d) J. Gallego, G. Varani, *Acc. Chem. Res.* **2001**, *34*, 836–843; e) E. E. Swayze, E. A. Jefferson, K. A. Sannes-Lowery, L. B. Blyn, L. M. Risen, S. Arakawa, S. A. Osgood, S. A. Hofstadler, R. H. Griffey, *J. Med. Chem.* **2002**, *45*, 3816–3819; f) Q. Vicens, E. Westhof, *ChemBioChem* **2003**, *4*, 1018–1023; g) J. R. Thomas, P. J. Hergenrother, *Chem. Rev.* **2008**, *108*, 1171–1224.
[7] V. W. Pollard, M. H. Malim, *Annu. Rev. Microbiol.* **1998**, *52*, 491–532.
[8] a) M. H. Malim, J. Hauber, S. Le, J. V. Maizel, B. R. Cullen, *Nature* **1989**, *338*, 254–257; b) U. Fischer, J. Huber, W. C. Boelens, I. W. Mattaj, R. Lührmann, *Cell* **1995**, *82*, 475–483; c) J. L. Battiste, H. Mao, N. S. Rao, R. Tan, D. R. Muhandiram, L. E. Kay, A. D. Frankel, J. R. Williamson, *Science* **1996**, *273*, 1547–1550.
[9] a) K. A. Lacourciere, J. T. Stivers, J. P. Marino, *Biochemistry* **2000**, *39*, 5630–5641; b) K. Moehle, Z. Athanassiou, K. Patora, A. Davidson, G. Varani, J. A. Robioson, *Angew. Chem.* **2007**, *119*, 9260–9264; *Angew. Chem. Int. Ed.* **2007**, *46*, 9101–9104; c) C. Pannecouque, D. Daelemans, E. D. Clercq, *Nat. Protoc.* **2008**, *3*, 427–434.
[10] a) S. Zheng, Y. Chen, C. P. Donahue, M. S. Wolfe, G. Varani, *Chem. Biol.* **2009**, *16*, 557–566; b) Y. Liu, E. Peacey, J. Dickson, C. P. Donahue, S. Zheng, G. Varani, M. S. Wolfe, *J. Med. Chem.* **2009**, *52*, 6523–6526.
[11] M. Maiti, G. S. Kumar, *Med. Res. Rev.* **2007**, *27*, 649–695.
[12] a) J. D. Puglisi, R. Tan, B. J. Calnan, A. D. Frankel, J. R. Williamson, *Science* **1992**, *257*, 76–78; b) C. Oubridge, N. Ito, P. R. Evans, C.-H. Teo, K. Nagai, *Nature* **1994**, *372*, 432–438; c) R. N. De Guzman, Z. R. Wu, C. C. Stalling, L. Pappalardo, P. N. Borer, M. F. Summers, *Science* **1998**, *279*, 384–388; d) P. Legault, J. Li, J. Mogridge, L. E. Kay, J. Greenblatt, *Cell* **1998**, *93*, 289–299; e) D. E. Draper, *J. Mol. Biol.* **1999**, *293*, 255–270.
[13] a) K. A. Abdullah, T. J. Kemp, *J. Photochem.* **1986**, *32*, 49–57; b) J. C. Dalton, F. C. Montgomery, *J. Am. Chem. Soc.* **1974**, *96*, 6230–6232.
[14] a) T. C. S. Pace, S. L. Monahan, A. I. MacRae, M. Kaila, C. Bohne, *Photochem. Photobiol.* **2006**, *82*, 78–87; b) S. H. Szajnman, W. Yan, B. N. Bailey, R. Docampo, E. Elhalem, J. B. Rodriguez, *J. Med. Chem.* **2000**, *43*, 1826–1840.
[15] a) C. P. Falshaw, N. A. Hashi, G. A. Taylor, *J. Chem. Soc. Perkin Trans. 1* **1985**, 1837–1843; b) N. Koumura, E. M. Geertsema, M. B. van Gelder, A. Meetsma, B. L. Feringa, *J. Am. Chem. Soc.* **2002**, *124*, 5037–5051.
[16] a) Z.-X. Wang, *FEBS Lett.* **1995**, *360*, 111–114; b) Z.-X. Wang, R.-F. Jiang, *FEBS Lett.* **1996**, *392*, 245–249.

Received: December 15, 2011
Revised: April 4, 2012
Published online: ■■ ▮▮, 0000

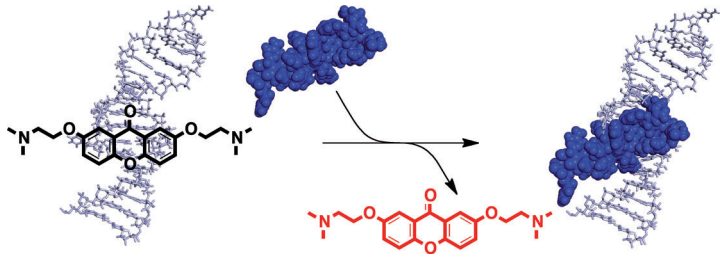

Indicating RNA binding: A fluorescent indicator displacement assay using 2,7-bis(aminoethoxy)xanthone (X2S) as the indicator is reported, for the study of small-molecule–RNA interactions (see figure). The substituents at the two alkoxy moieties modulate the binding selectivity. The X2S derivative having *N*,*N*-dimethylaminoethoxy substituents is the best fluorescent indicator in the screening of molecules binding to Rev response element (RRE).

Fluorescent Probes

*S. Umemoto, S. Im, J. Zhang, M. Hagihara, A. Murata, Y. Harada, T. Fukuzumi, T. Wazaki, S. Sasaoka, K. Nakatani** ..... ▮▮▮▮–▮▮▮▮

Structure–Activity Studies on the Fluorescent Indicator in a Displacement Assay for the Screening of Small Molecules Binding to RNA